


RESEARCH ARTICLE

Comparative Metabolic Profiling of Wild and In Vitro Cultivated *Cecropia angustifolia* Roots Fraction Reveals Conservation of Pentacyclic Triterpene Acid Biosynthesis

Luis M. Díaz-Sánchez^{1,2} | Martha L. Chacón-Patiño³ | Cristian Blanco-Tirado¹ | Marianny Y. Combariza¹ | Guillermo Montoya^{4,5} 

¹Escuela de Química, Universidad Industrial de Santander, Bucaramanga, Santander, Colombia | ²Departamento de Química, Universidad de Pamplona, Pamplona, Norte de Santander, Colombia | ³National High Magnetic Field Laboratory, Florida State University, Tallahassee, Florida, USA | ⁴BioInc. Center for Biomass Valorization Research, Universidad Icesi, Cali, Valle del Cauca, Colombia | ⁵Facultad Barberi de Ingeniería, Diseño y Ciencias Aplicadas. Escuela de Ciencias Aplicadas e Industria Sostenible, Departamento de Ciencias Farmacéuticas y Químicas, Universidad Icesi, Cali, Valle del Cauca, Colombia

Correspondence: Luis M. Díaz-Sánchez (luis.diazsanchez@unipamplona.edu.co) | Marianny Y. Combariza (marianny@uis.edu.co) | Guillermo Montoya (glmontoya@icesi.edu.co)

Received: 20 January 2025 | **Revised:** 2 June 2025 | **Accepted:** 10 June 2025

Funding: This work was supported by the Ministry of Science, Technology, and Innovation of Colombian Government (Grants 430-2020 code number 211784467730 and 435-2021) and Universidad ICESI (Grant Number CA04130107).

Keywords: *Cecropia angustifolia* | pentacyclic triterpenes | ultrahigh-resolution mass spectrometry

ABSTRACT

Introduction: *Cecropia angustifolia* roots are a traditional source of pentacyclic triterpene acids (PTAs), bioactive compounds with promising therapeutic potential. In vitro cultivation offers a sustainable alternative to metabolite production while minimizing the impact on wild populations.

Objective: To compare the metabolic profiles of wild and in vitro cultivated *C. angustifolia* roots using ultrahigh-resolution mass spectrometry.

Methods: Root fractions from wild and in vitro cultivated materials were analyzed using negative-ion electrospray ionization Fourier transform ion cyclotron resonance mass spectrometry (ESI(−)-FT-ICR-MS) at 21 Tesla.

Results: Molecular analysis revealed diverse PTA species in both wild and in vitro root fractions. While in vitro cultivation produced a more streamlined metabolic profile, PTA content remained significantly enriched.

Conclusion: In vitro cultivation of *C. angustifolia* roots represents a viable strategy for sustainably producing pharmacologically relevant PTAs, supporting both conservation and the biotechnological use of natural products.

1 | Introduction

Cecropia angustifolia Trécul (Urticaceae) is a pioneer species native to neotropical habitats, thriving in montane humid regions across Central and South America, including Guatemala, Honduras, Nicaragua, Costa Rica, Panama, Colombia, Venezuela, Ecuador, and Peru. In addition to its medicinal value, this species plays an important ecological role by supporting

pollinators and contributing to the health of rainforest ecosystems. However, *C. angustifolia* is increasingly threatened by habitat loss, highlighting the need for its conservation and sustainable use [1].

The roots of *C. angustifolia* have long been recognized for their bioactive properties, with pharmacological studies demonstrating the potential to modulate inflammation, improve insulin

sensitivity, and reduce glucose resistance [2, 3]. Among the plant's phytochemicals, pentacyclic triterpene acids (PTAs), derived from oleanane and ursane skeletons, stand out as key chemical markers due to their notable therapeutic potential. Although typically present in low abundance in plants, these secondary metabolites are widely reported for their health benefits, particularly in managing obesity and metabolic syndrome [4–7]. Modern biotechnological approaches offer opportunities to harness biodiversity and enhance the availability of such natural compounds, paving the way for sustainable and rational therapies targeting complex diseases [8, 9].

Advances in Fourier transform ion cyclotron resonance mass spectrometry coupled with electrospray ionization (ESI FT-ICR-MS) have enabled the comprehensive profiling of plant metabolomes, allowing for the detection of thousands of metabolites with ultrahigh mass accuracy and resolving power. Ultrahigh-resolution mass spectrometry (UHRMS) is widely employed in metabolomics due to its unmatched capability to analyze all ionizable compounds in complex biological matrices without prior separation. This technique excels at revealing subtle metabolic changes associated with biotic and abiotic stress, elucidating biosynthetic pathways, and facilitating the discovery of novel nutraceutical compounds [10, 11]. These advantages make FT-ICR-MS a powerful tool for untargeted metabolomics, enabling deep chemical characterization that is often unattainable with other analytical methods.

Moreover, in vitro cultivation has emerged as a promising biotechnological alternative for producing bioactive compounds from non-domesticated plants. This approach, based on tissue culture technologies, an established yet continually evolving field, allows for the replication of natural biosynthetic pathways while minimizing land and resource use [8, 12]. These strategies are particularly important for accessing low-abundance metabolites such as PTAs. Nonetheless, uncertainties remain regarding the extent to which in vitro cultivation influences the metabolic profile of these compounds.

This study represents a significant advance by applying ESI(–) 21T FT-ICR-MS to compare the metabolic profiles of wild and in vitro cultivated *C. angustifolia* roots. Unlike previous reports limited to detecting only a few compounds, this untargeted metabolomic approach allows comprehensive identification of bioactive metabolites, highlighting both similarities and differences in molecular composition and offering deeper insights into PTA biosynthesis. Furthermore, this work demonstrates how combining biotechnology with advanced analytical techniques supports the sustainable and targeted production of pharmacologically relevant metabolites, reinforcing the potential of in vitro culture as an ecological alternative for the conservation and utilization of plant resources.

2 | Materials and Methods

2.1 | Herbal Material and Fraction Preparation

Roots of *C. angustifolia* were collected in July 2021 from Pance, Valle del Cauca, Colombia (geographic coordinates: 3°20'12.0" N, 76°38'41.6" W; altitude: 1771 m). The plant

material was authenticated by comparison with voucher specimen OD2126 deposited at the herbarium of Universidad Icesi. Access to genetic resources was granted under Agreement No. 180 between Universidad Icesi and the Colombian Ministry of Environment (Addendum No. 10), issued on May 7, 2018. All procedures complied with the Nagoya Protocol.

The plant material was dried at 40°C for three consecutive days and then ground using a hammer mill. Extraction was performed using a 1:1 mixture of ethyl acetate (EA) and dichloromethane (DCM) at a 1:10 ratio of herbal material to solvent. The mixture was stirred at 90 rpm at room temperature for 72 h. The residue was removed by filtration, and the solvent was recovered and evaporated to dryness. The resulting extract was subjected to vacuum chromatography under normal-phase conditions using EA to isolate the fraction enriched in PTAs. The solvent was then removed under vacuum, yielding a pale-yellow amorphous powder.

2.2 | In Vitro Cultivation System for Fraction Production

The protocol for in vitro cultivation fraction was previously reported using indole-3-butyric acid to root from a 6-month-old callus tissue [3]. A total of 0.5 g of *C. angustifolia* callus was weighed and placed into sterile petri dishes, close to 30 days after small roots from the callus material were recognized, and the process stopped 3 months later. All the material was cleaned from media, dried, and processed under the fraction preparation protocol.

2.3 | Pentacyclic Triterpene Content Quantification by Selecting Ion Recording

The production of serjanic acid reported by our lab in *Cecropia telenitida* gives us the possibility to use it as an internal standard $[M-H]^-$ m/z 499 to control the production of relative quantitative expression [13] because this PTA is not quantifiable by our readout system and was only detected by UHRMS with a low abundance (see Figures S3 and S4 and Tables S1 and S2). To simplify the analysis, and considering the fraction contains many isobaric triterpenes, it was decided to select the mass-to-charge ratio $[M-H]^-$ m/z 487 represented by the most oxidized molecules, like yarumic, isoyarumic, arjunolic, or tormentic acids. $[M-H]^-$ m/z 471 is represented by molecules like hederagenic and 20-hydroxy-ursolic, maslinic, and corosolic acids. The precursors of the mentioned molecules come from less oxidized oleanyl and ursanyl cations $[M-H]^-$ m/z 455 represented by oleanolic and ursolic acids. A specific amount of dry fraction is solubilized in a volumetric flask and diluted to prepare a $10 \mu\text{g mL}^{-1}$ then filtrated into chromatographic vials for UPLC-MS analysis.

Analysis and quantitation were carried out in a UPLC-SQD2 mass spectrometry Waters. The chromatographic separation of triterpene acids was carried out on Acquity UPLC BEH C18 (100×2.1 mm, $1.7 \mu\text{m}$) and the column was kept at 35°C. The mobile phase was Milli-Q water with 5 mM of ammonium acetate (A) and methanol hypergrade (B) at constant flow rate of

0.3 mL min⁻¹ with a gradient elution of 0 min at 30% A, 1 min at 20% A, 1.50 min 15% A, 3 min 5% A, 4.50 min 2% A, 6.00 min 2% A, and 10 min 30% A.

The mass spectrometer uses an electrospray ionization (ESI) source, kept at 500°C and acquired in negative mode. Nitrogen was used as a nebulizer and curtain gas. The optimal values for MS parameters were capillary voltage 3.50 kV, cone voltage 80 V; desolvation temperature 500°C and desolvation gas source flux 900 L/h. The analyzer was operated in single ion recording (SIR) acquisition mode, which monitored [M-H]⁻ ions at *m/z* of 487, 455, and 471, and additionally serjanic acid as the IS at *m/z* 499. Masslynx MS Software was used for instrument control, data acquisition, as well as data processing.

2.4 | Metabolic Profile Evaluation

The fraction from both wild and in vitro cultivated *C. angustifolia* root materials were diluted at a ratio of 1:1000 in ultrahigh-purity HPLC-grade methanol (J.T. Baker, Phillipsburg, NJ), with 0.1% NH₄OH, before undergoing analysis via 21T FT-ICR-MS at the National High Magnetic Field Laboratory (NHMFL), Florida State University. Analysis was conducted in negative ESI mode using a custom-built hybrid linear ion trap FT-ICR mass spectrometer equipped with a 21T superconducting solenoid magnet. Mass spectra underwent phase correction and internal calibration using a set of 10–15 highly abundant homologous series spanning the entire molecular weight distribution (~150 calibrant peaks) via the walking calibration method. Peaks exceeding six times the baseline root-mean-square (rms) noise at *m/z* 400 were exported as peak lists. Molecular formula assignments and data visualization were performed using PetroOrg software developed by the NHMFL Lab and GraphPad Prism 10.4. Molecular formulas were assigned based on specific parameters, encompassing elemental compositions of C_{0 to 100}, H_{0 to 100}, and O_{0 to 20}, along with a maximum hydrogen-to-carbon ratio of 2, and a double bond equivalent (DBE) value of 30. Assignments exceeding a mass accuracy of 0.2 parts per million (ppm) were excluded.

3 | Results and Discussion

The neotropical realm possesses similar flora across rainforest ecoregions, making it one of the most important biodiversity reserves. *C. angustifolia* is a montane tree native to Central and South America, with a higher distribution in Colombia and Ecuador on both sides of the Andes (Figure 1A) [1]. In Colombia, the three branches of the Andes, known as the cordilleras, stretch from southwest to northeast, creating pronounced topographic gradients that shape distinct biogeographical regions where species diversification naturally occurs [14]. Despite its ecological importance, phytochemical information on this species remains limited, and conservation efforts have focused on biomass production through biotechnological approaches.

Previous reports comparing the most abundant triterpenes between in vitro cultivated and wild materials revealed a shift in dominant oxidized PTAs [3]. Wild roots (Figure 1C) exhibited higher levels of oxidized PTAs, while in vitro cultivated roots

(Figure 1B) showed reduced quantities. Thin-layer chromatography (TLC) analysis confirmed a high triterpene content and revealed additional phytochemicals (Figures S1–S3). Subsequent fractionation via normal-phase flash chromatography yielded PTA-enriched fractions (>56% dry weight) from both sources, including a glycosylated compound with *m/z* 633, identified as a glycosylated derivative of *m/z* 471 with the molecular formula C₃₆H₅₈O₉ (Tables S1 and S2). PTAs were quantified using single ion recording (SIR) acquisition mode in UPLC-SQD2 with serjanic acid (*m/z* 499 [M-H]⁻) as the internal standard (Figure S4). The PTAs profiles differed significantly between wild and in vitro cultivated roots, as shown in Figure 2A,B. For instance, four isomers at *m/z* 471 were detected in wild roots (Figure 2A), with Peaks 3 and 4 showing high ion abundance and Peak 2 notably reduced in in vitro roots (Figure 2B). Similarly, four isomers at *m/z* 487 were observed in wild material, with Peak 3 exhibiting comparable intensity in both root types. These isobaric PTAs have been previously characterized by our group using NMR [13, 15, 16]. Notably, ultra-high mass resolving power is essential for detailed analysis of PTA's metabolic profiles to differentiate between nominal isobaric compounds.

The ultra-high resolving power and mass accuracy of the 21T FT-ICR MS facilitate comprehensive molecular formula determination across all ionizable compounds in complex biological matrices [17]. Figure 2 presents the ESI negative mode FT-ICR mass spectra of wild (Figure 2C) and in vitro cultivated (Figure 2D) fractions within the *m/z* 180–1200 mass range (Figure S5). Data filtration yielded a non-assigned peak percentage (no-hit) of 7.7% for the wild root fraction and 3.4% for the in vitro cultivated root fraction. One thousand twenty-two compounds were identified in wild roots and 439 in in vitro cultivated roots, with signal-to-noise ratio (S/N) > 6. The experimental resolving power was 1.3 × 10⁶ at *m/z* 400, achieved by co-adding 100 scans, each representing ion signals from approximately 1 × 10⁶ charged species [18]. Table 1 summarizes the suggested [M-H]⁻ molecules derived from the metabolic decoration of ursane and oleanane skeletons, cross-referenced with NMR reports and PetroOrg software data [19]. The complete table with 1461 detected ions and their molecular formulas is included in the [Supporting Information](#). The mass errors in Table 1 are presented in parts per billion (ppb), ensuring high confidence in molecular formula assignments.

Interestingly, the highest double bond equivalent (DBE) values increased in correlation with the number of oxygen atoms (Figure 3B–E), likely influenced by C=O bonds that are not directly included in DBE calculations [20]. Most compounds in the O₃ (o=3–5) class were common in both sources. Yet, in the in vitro cultivated fraction, the O₄ (Figure 3C) and O₆ (Figure 3E) plots reveal compounds with the highest DBE values of 13 and 19, respectively. The above indicates that more unsaturated compounds are formed in the in vitro cultivated roots. These unsaturated structures are located within the lower left-hand quadrant of the van Krevelen diagram (Figure 3A). The DBE versus carbon number plots also revealed the presence of dimeric ions, e.g., [M₁ + M₂-H]⁻ ions with M₁ C₃₀H₄₈O₃ and M₂ C₃₀H₄₈O₄ at *m/z* 927.70832 (relative abundance of 1.90), and [M₂ + M₃-H]⁻ ions with M₂ C₃₀H₄₈O₄ and M₃ C₃₀H₄₈O₅ at *m/z* 959.69817 (relative abundance of 1.75). Notably, [M-H]⁻ and [2M-H]⁻ ions of C₃₀H₄₈O₃ were detected at *m/z* 455.35284 (relative

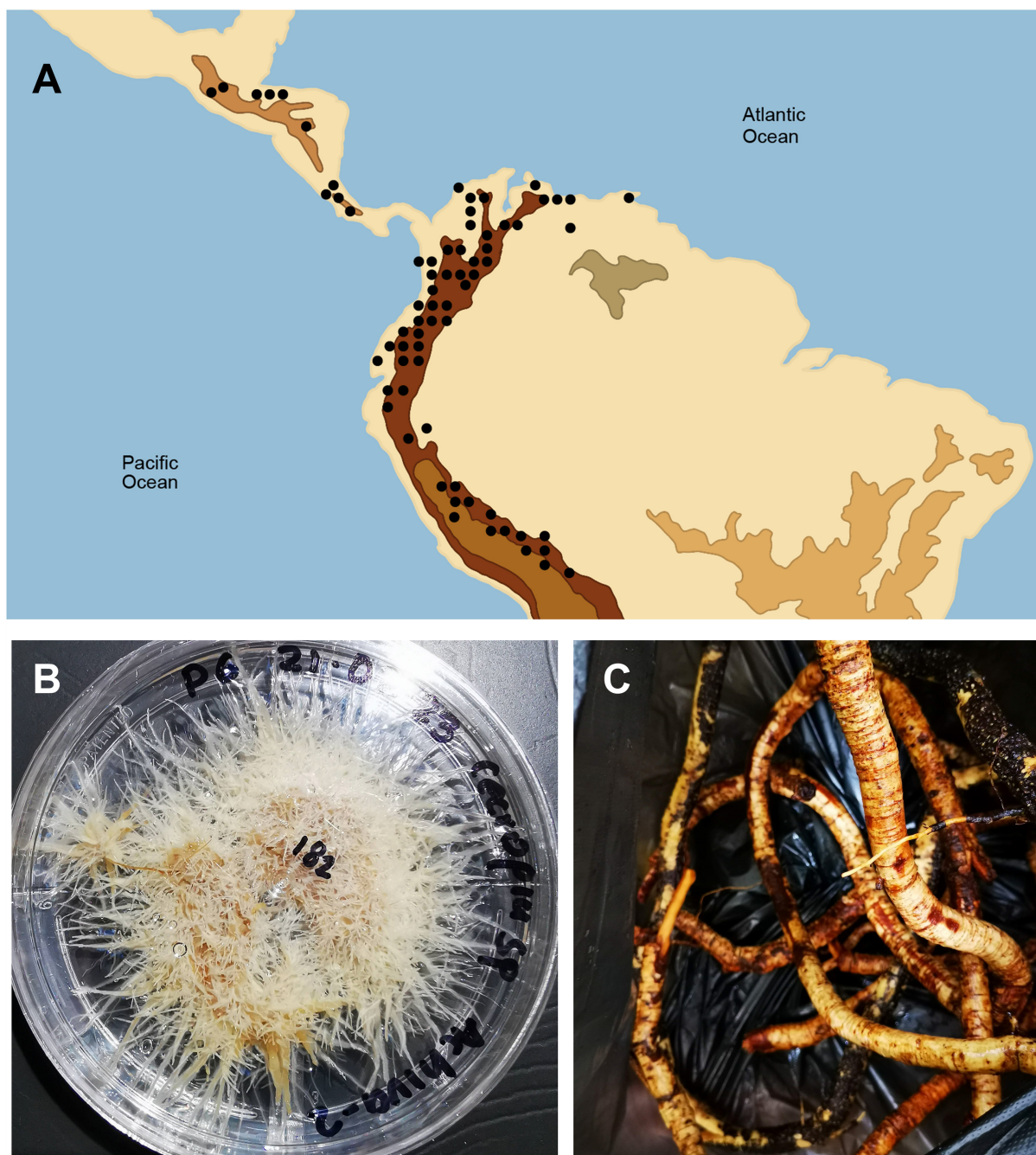


FIGURE 1 | Distribution map of *C. angustifolia* in South and Central America (A) [1], *C. angustifolia* in vitro root culture (B), and wild root material collected in the National Natural Park Farallones de Cali, Valle del Cauca, Colombia (C).

abundance of 52.30) and m/z 911.71341 (relative abundance of 0.92). Additionally, for compound $C_{30}H_{50}O_3$, monomeric and dimeric species were observed at m/z 457.36872 and m/z 915.74471. Dimers can form in ESI due to molecular interactions in the ion source, and their detection provides valuable structural information, aiding in molecular formula assignment.

Analyzing compound classes allows for the discovery of new ones within the same homologous series (horizontal line), driven by variations in CH_2 units. Additionally, differences along the vertical line between points may correspond to variations in the number of double bonds (a difference of H_2) in the molecular structures. PTAs, featuring five rings and two or three double

bonds in their structures, typically fall within a specific range of DBE values of 7 or 8 (Figure 3B–E). General formulas were established for the homologous series $C_nH_{2n-12}O_3$, based on the number of oxygen atoms in each class. In the O_3 class, ursolic acid $C_{30}H_{46}O_3$ with DBE 8 was detected, which is part of a two-member series detected only in the in vitro cultivated fraction of *C. angustifolia* roots. In contrast, ursolic acid $C_{30}H_{48}O_3$ with DBE 7 is part of a four-member series with the general formula $C_nH_{2n-12}O_3$, where $C_{29}H_{46}O_3$ has been previously reported by other authors as a PTA-derived analog [21]. In the O_5 class, serjanic acid $C_{31}H_{48}O_5$ with DBE 8 was detected in low abundance and used as an internal standard for relative quantitation whose ESI-FT-ICR-MS spectrum is shown in Figure S4. Following

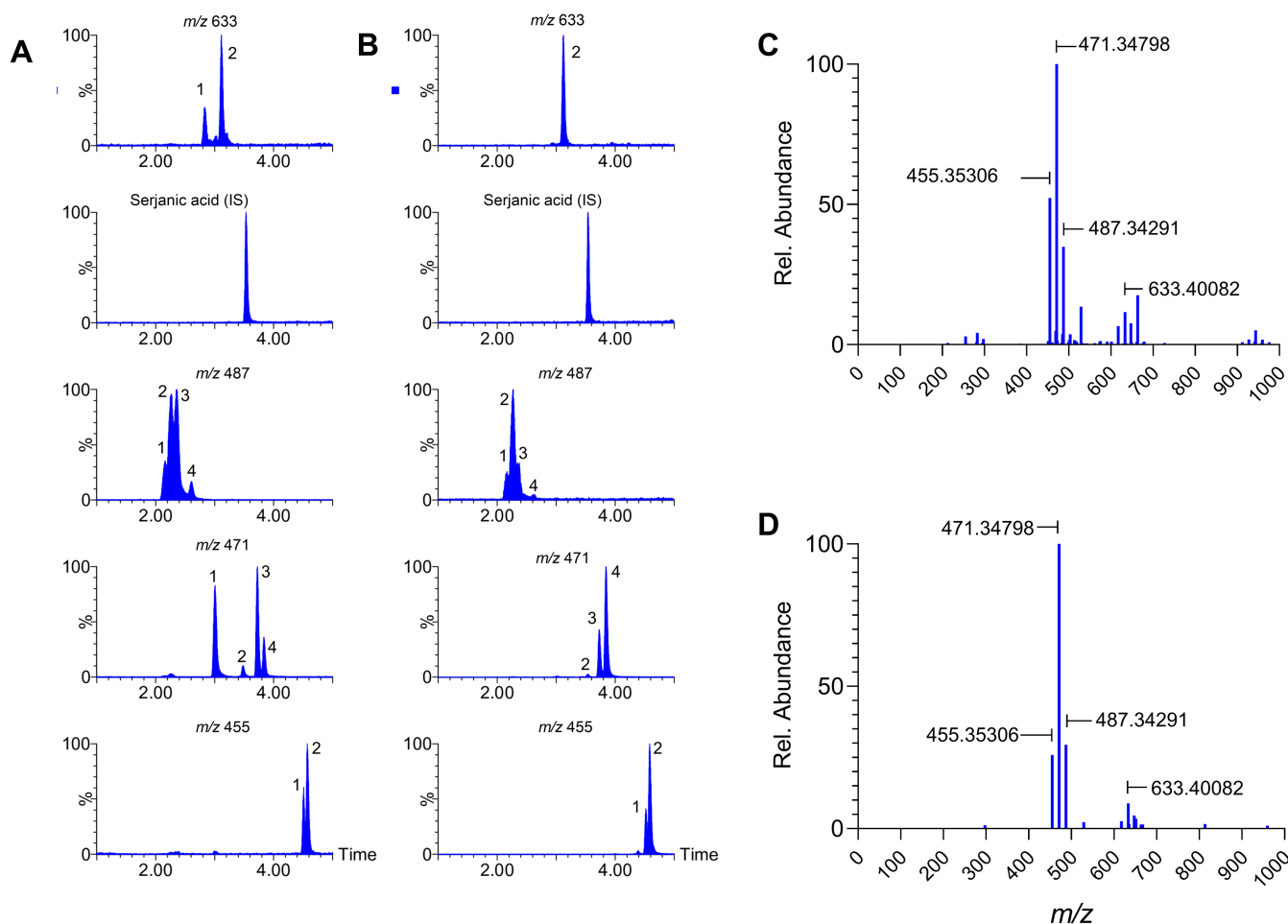


FIGURE 2 | UPLC-SQD2 single ion recording (SIR) acquisition mode chromatograms for wild (A) and in vitro cultivated (B) PTAs fraction with monoisotopic masses at m/z 455, 471, 487, and 633, using serjanic acid as internal standard. ESI(−) 21T FT-ICR-MS spectra of wild (C) and in vitro cultivated (D) *C. angustifolia* root fractions.

the biogenetic rules of *C. angustifolia*, a molecular structure was proposed for the assigned formula $C_{30}H_{46}O_5$. Additionally, molecular structures are proposed in this study for some compounds of the DBE 7 and 8 homologous series in the O_6 class. The proposed molecular structures are detailed in Figure S6. The assigned and proposed compounds may have isomers that could not be distinguished in this study.

The molecular profiles in Figure 2A are consistent with earlier analyses using the ESI-ion trap (ESI-IT) and matrix-assisted laser desorption/ionization-time of flight (MALDI-TOF) of *Cecropia* root extracts [3, 13]. Molecular formulas $C_{30}H_{48}O_3$, $C_{30}H_{48}O_4$, and $C_{30}H_{48}O_5$ dominated both fractions, with m/z 455, 471, and 487 peaks collectively representing >80% of detected ions. The UHRMS analysis confirmed previous findings but revealed additional complexity with 1461 different compounds identified. Ursolic ($C_{30}H_{48}O_3$), goreishic I ($C_{30}H_{46}O_4$), 20-hydroxyursolic ($C_{30}H_{48}O_4$), isoyarumic ($C_{30}H_{48}O_5$), and serjanic ($C_{31}H_{48}O_5$) acids, along with glycosylated analogs, were detected in the high-mass region (Figure 2A,B, Table 1). Glycosides of four previously reported PTAs were also identified.

Oxygenated pentacyclic triterpenes, such as alcohols, ketones, ethers, and carboxylic acids, result from cytochrome P450 (CYP450) oxidases modifications during the biosynthesis of

PTAs [22–24]. Oxidations at C28, C23, 2α , 19α , 20β , and double bonds in carbon atoms 11, 12, and 17 generate structural diversity, as shown in the proposed pathway (Figure 4). While biosynthetic pathways remain active in both environments, natural growing conditions yield broader molecular diversity due to environmental stressors, soil composition, and microbial interactions [25].

UHRMS enables comprehensive profiling of complex biological samples, tracking precursor conversion through enzymatic reactions, including oxidation and hydroxylation steps. Wild and in vitro cultivated roots exhibited higher relative abundances for classes O_0 ($o=3, 4$, and 5). The O_4 class dominated both fractions, with a higher abundance in wild roots. The van Krevelen diagram (Figure 3A) revealed more saturated compounds (H/C 1.7–1.9) and higher oxygen content (O/C up to 0.7) in wild material, likely due to glycosylated derivatives. In vitro cultivation produced fewer complex extracts, simplifying target compound extraction. In ESI(−), the metabolic profiles of both samples correspond to 14 compound classes of oxygenated species O_0 ($o=2$ –15), out of which 12 were common to both wild and in vitro cultivated cultures (Figure 5A,B).

Compounds in O_0 ($o=2$ –8) classes exhibited higher relative abundances than O_0 ($o=9$ –15), suggesting aglycones dominate

TABLE 1 | Some compounds detected by cross-referenced NMR reports and PetroOrg as [M-H]⁻ in the ESI FT-ICR MS mass spectra of wild and in vitro cultivated *C. angustifolia* root fractions.

ESI FT-ICR MS									
Compound	Molecular formula	m/z theor.	Wild material			In vitro material			
			m/z experimental	Mass accuracy (ppb)	Relative abundance	m/z experimental	Mass accuracy (ppb)	Relative abundance	Relative abundance
Oleanonic (ursonic) acid	C30H46O3	453.33742				453.33741	20		0.70
Ursolic acid	C30H48O3	455.35306	455.35306	19	52.31	455.35306	20		25.98
Oleanolic acid	C30H48O3	455.35307	455.35306	19	52.31	455.35306	20		26
Goreishic acid I	C30H46O4	469.33233	469.33233	7	4.91	469.33233	7		0.74
Maslinic (corosolic, 20-hydroxy-ursolic, hederagenic) acid	C30H48O4	471.34798	471.34798	7	100	471.34798	8		100.49
3-keto-isoyarumic acid	C30H46O5	485.32725	485.32725	4	3.80	485.32725	4		0.9479
Unknown 1	C31H50O4	485.36363	485.36365	34	0.04	485.36368	96		0.0169
Isoyarumic (yarumic, tormentic, arjunolic) acid	C30H48O5	487.34290	487.34291	24	34.86	487.34291	24		29.5686
Unknown 2	C31H46O5	497.32725	497.32726	24	0.11	497.32726	24		0.0202
Serjanic acid	C31H48O5	499.34289	499.34291	23	0.27	499.34292	43		0.02
Unknown 3	C30H46O6	501.32216	501.32217	14	1.71	501.32217	14		0.4192
Unknown 4	C30H48O6	503.33781	503.33782	14	3.70	503.33782	14		0.717
Unknown 5	C32H48O5	511.34290	511.34289	16	0.05				
Unknown 6	C30H42O7	513.35855	513.35856	25	0.04				
Unknown 7	C31H48O6	515.33781	515.33782	14	0.43	515.33782	14		0.0637
Unknown 8	C31H50O6	517.35346	517.35347	14	1.18	517.35347	14		11.78
Unknown 9	C32H48O6	527.33781	527.33782	14	0.23	527.33781	5		0.0177
Unknown 10	C32H50O6	529.35346	529.35347	13	13.52	529.35347	13		22.997
Unknown 11	C31H48O7	531.33273	531.33274	24	0.10	531.33275	42		0.0178
Unknown 12	C33H52O8	575.35894	575.35896	31	0.15	575.35894	4		0.0259
3-Glc-β-amyrin	C36H60O6	587.43171	587.43176	80	0.05	587.43169	39		0.023

(Continues)

TABLE 1 | (Continued)

Compound	ESI FT-ICR MS							
	Molecular formula	m/z theor.	Wild material			In vitro material		
			m/z experimental	Mass accuracy (ppb)	Relative abundance	m/z experimental	Mass accuracy (ppb)	Relative abundance
Oleanolic-3-O-glucopyranoside	C36H58O8	617.40589	617.40591	29	0.20	617.4059	12	0.085
Goreishic-3-O-glucopyranoside	C36H56O9	631.38516	631.38517	21	0.06	631.38524	132	0.0121
(20-hydroxyursolic, hederagenin, corosolic, maslinic)-3-O-glucopyranoside	C36H58O9	633.40081	633.40082	21	0.11	633.40082	21	0.1737
Unknown 13	C36H56O10	647.38007	647.38012	75	0.03			
(Arjunolic, yarumic, isoyarumic, tormentic)-3-O-glucopyranoside	C36H58O10	649.39572	649.39573	13	0.07	649.39573	13	0.0988
28beta-Glc-madecassic acid	C36H58O11	665.39064	665.39065	21	0.07	665.39065	21	0.166
Unknown 14	C36H58O12	681.38555	681.38552	45	0.03	681.38555	1	0.0506
3-glc-23-glc-hederagenin	C42H68O14	795.45363				795.45363	1	0.0243

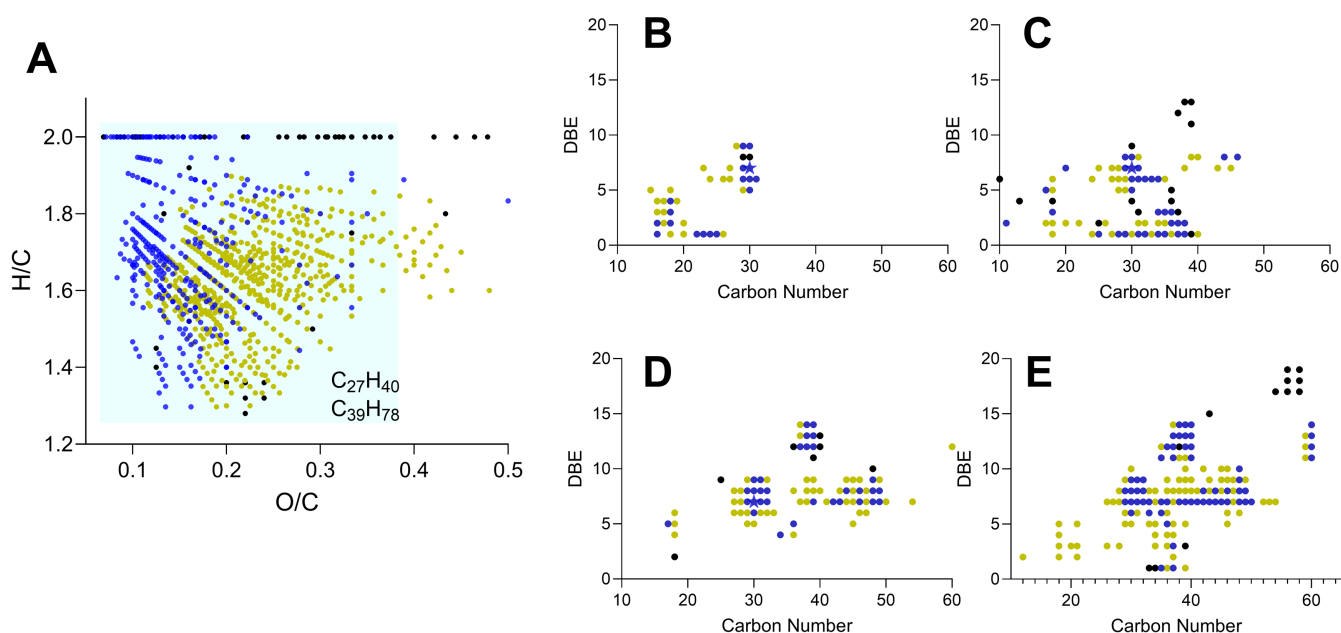


FIGURE 3 | van Krevelen diagram overlay showing H/C and O/C ratios of assigned formulas in wild (olive), in vitro cultivated (black), and both fractions (blue) (A). DBE versus carbon atom number plots for O_3 (B), O_4 (C), O_5 (D), and O_6 (E) compound classes.

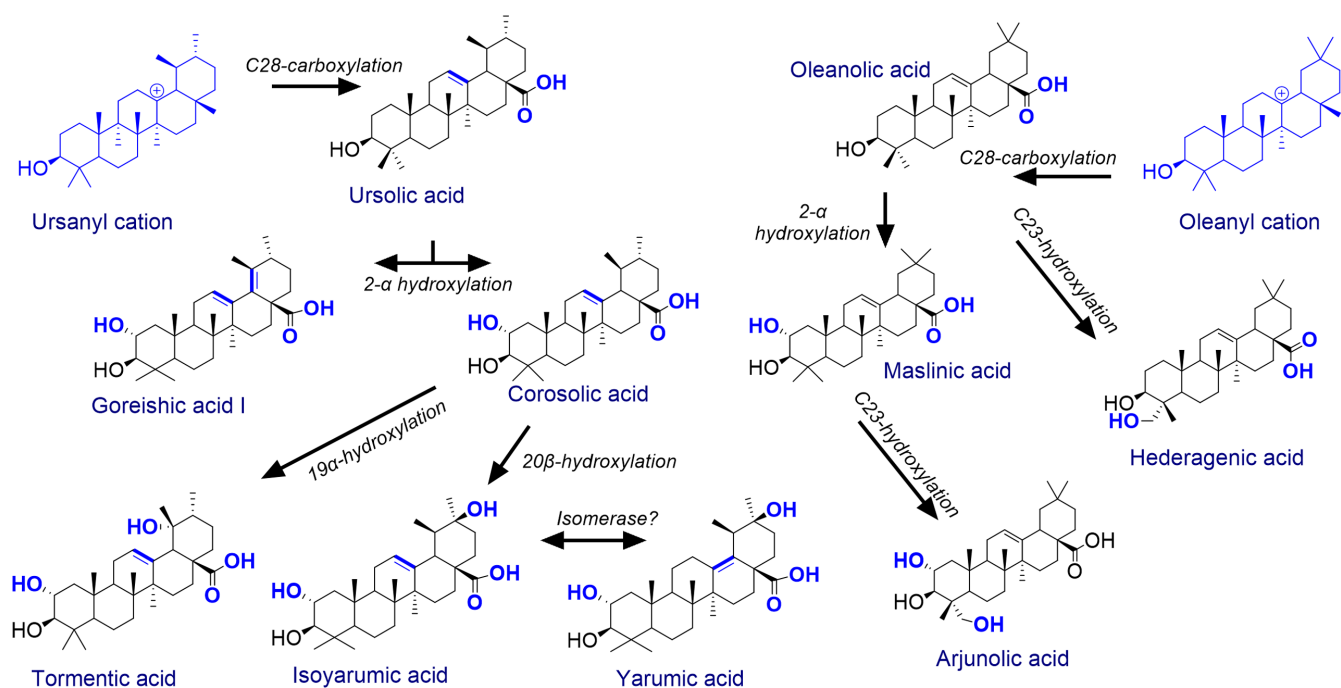


FIGURE 4 | Metabolic pathway for PTA biosynthesis in *C. angustifolia*. CYP450 oxidases decorate triterpene templates by oxygenating C2, C19, C20, C23, and C28 [24].

over glycosylated PTAs in extracts. This aligns with trends observed in Asteraceae species [26]. Environmental factors and growth conditions influence aglycone-glycoside ratios [27]. The DBE versus carbon number plots (Figure 3B–E) revealed unsaturated compounds with higher DBE values in vitro cultivation. For example, the O_4 and O_6 classes displayed maximum DBE values of 13 and 19, respectively, suggesting the formation of more unsaturated structures in vitro cultivation.

Triterpene oxidation is essential for structural diversification, directly influencing its biological properties. The distribution of compound classes reveals a comparable pattern in fractions from both growth conditions (Figure 5A), indicating that critical biosynthetic pathways remain active regardless of the specimen's origin. The most abundant compound classes are characterized by O_3 , O_4 , and O_5 compound classes, which dominate in both wild and in vitro cultivated conditions (Figure 5B). As indicated above, UHRMS offers unmatched

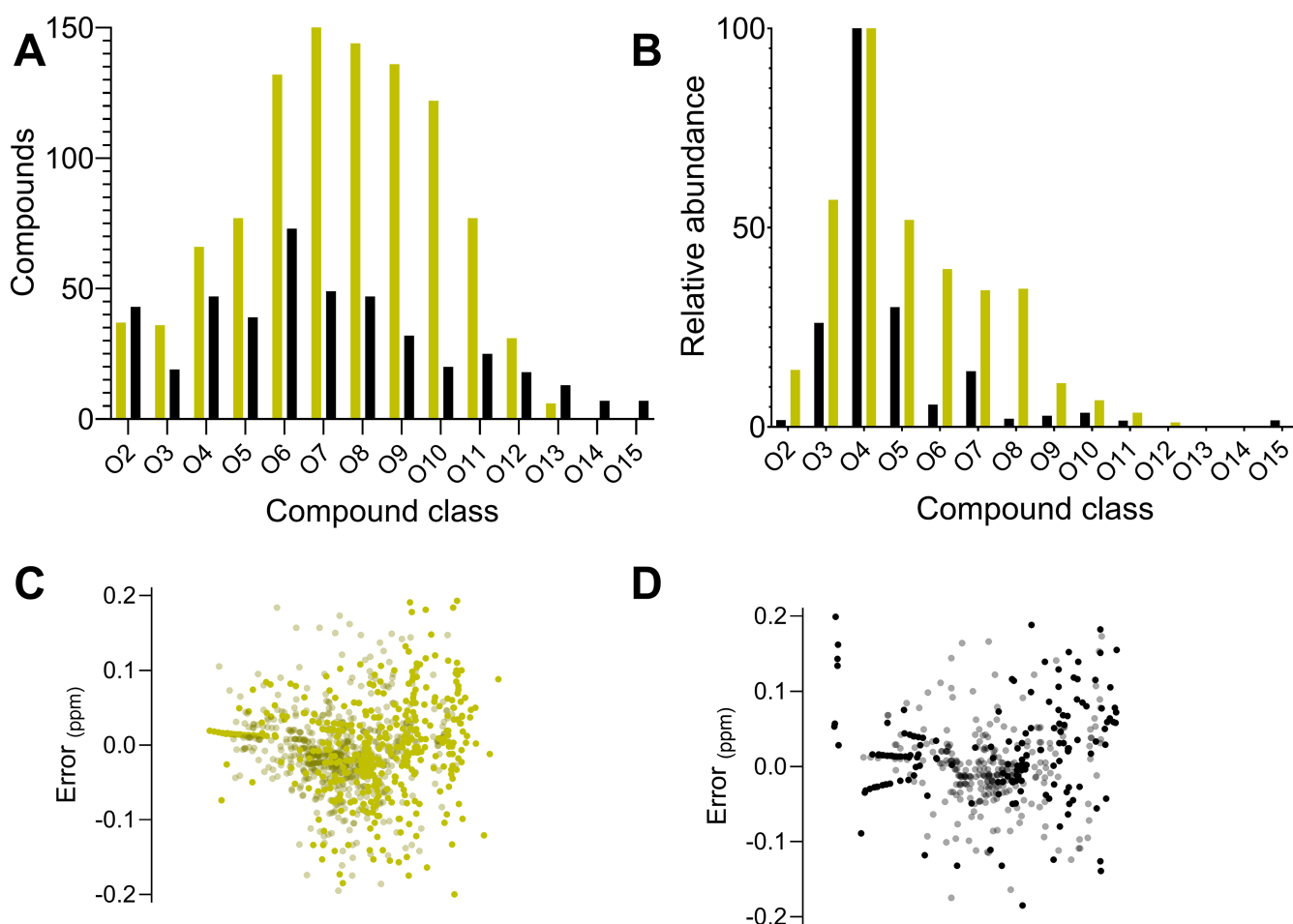


FIGURE 5 | Comparative histograms showing the distribution of molecular formulas categorized by oxygenation level (A) and compound classes based on ion abundances (B) in the wild and in vitro cultivated *C. angustifolia* fractions. Scatter plots illustrate the mass error of FT-ICR-MS assigned formulas in wild (C) and in vitro cultivated (D) root materials. Decolorized points represent molecules with oxygenation levels ranging from O₃ to O₈ in both (C) and (D). Data points corresponding to wild roots are shown in olive color, while those from in vitro cultivated roots are displayed in black color.

precision in molecular mass measurement, allowing for confident molecular formula assignments with extremely low error margins as determined in wild (Figure 5C) and in vitro cultivated (Figure 5D) herbal material. Its high mass resolution and resolving power allow the separation of ions, which is critical for distinguishing compounds with nearly identical elemental compositions, providing comprehensive insights into chemical diversity and biosynthetic pathways. These results suggest that fundamental metabolic processes are preserved in both environments (Figure 4). Consequently, cultivating *C. angustifolia* roots under controlled conditions emerges as a promising strategy to reduce reliance on wild material for future research efforts while contributing to species conservation and ecosystem preservation.

4 | Conclusion

The wild and in vitro cultivated *C. angustifolia* roots exhibit conserved metabolic pathways, particularly those related to the biosynthesis of PTAs, a class of metabolites with significant pharmacological potential. However, notable differences in molecular complexity were observed, with wild roots showing

greater chemical diversity, likely influenced by environmental factors. Conversely, in vitro cultivated roots exhibited a streamlined metabolic profile, enriched in PTAs, indicating that this method can selectively enhance the production of bioactive compounds.

The reduced molecular diversity in in vitro cultivated roots, while limiting in terms of chemical heterogeneity, represents a significant advantage for targeted metabolite production, offering a scalable and sustainable approach to obtaining high-value compounds. This strategy supports conservation efforts by reducing the need for wild harvesting, thus preserving endangered habitats and contributing to biodiversity protection. Additionally, the integration of UHRMS in this study underscores the transformative potential of advanced analytical techniques to uncover the nuanced metabolic differences and structural details with high precision and accuracy.

One limitation of ESI-FT-ICR is its inability to differentiate isomers, as they share identical m/z values. This limitation was addressed in the present study using UPLC, as reported in previous research. However, considering the inherent limitations of UPLC—such as incomplete resolution of certain isomeric

compounds—future work could explore the application of ion mobility spectrometry (IMS) for extract analysis, which may contribute to definitively characterizing specific structural variants within the complex metabolite mixtures analyzed.

This research not only highlights the utility of in vitro cultivation for sustainable production but also establishes a foundation for exploring novel applications of *C. angustifolia* metabolites in pharmaceuticals, particularly for metabolic disorders such as type 2 diabetes. Future studies could delve deeper into optimizing in vitro cultivation conditions to further enhance the yield of specific bioactive compounds and elucidate the environmental and genetic factors driving metabolic variation. By fostering a synergy between conservation biology, cutting-edge biotechnology and mass spectrometry, this work advances the sustainable exploration and utilization of natural products for industrial and therapeutic applications.

Acknowledgments

We thank Guatiguará Technology Park at Universidad Industrial de Santander (UIS) for infrastructural support. Special acknowledgment to MINCIENCIAS (Grant Number 430-2020). A portion of this work was performed at the National High Magnetic Field Laboratory, supported by the National Science Foundation Cooperative Agreement No. DMR-2128556 and the State of Florida. FT-ICR MS data are publicly available at OSF, DOI [10.17605/OSF.IO/X5D47](https://doi.org/10.17605/OSF.IO/X5D47).

Data Availability Statement

The data that support the findings of this study are available in the supplementary material of this article.

References

1. C. C. Berg, P. F. Rosselli, and D. W. Davidson, "Cecropia," in *Flora Neotropica*, vol. 94 (New York Botanical Garden Press, 2005).
2. G. Gutiérrez, D. Giraldo-Dávila, M. Y. Combariza, et al., "Serjanic Acid Improves Immunometabolic Markers in a Diet-Induced Obesity Mouse Model," *Molecules* 25 (2020): 1486.
3. J. Vazquez-Delgado, J. Vivas-Moncayo, J. Lopez-Cortes, M. Combariza, and G. Montoya, "Pharmacokinetic Assessment and Phytochemical Triterpene Control From *Cecropia angustifolia* Using Plant Biotechnology," *Phytochemical Analysis* 34 (2023): 641–651.
4. S. Xu, G. Wang, W. Peng, et al., "Corosolic Acid Isolated From *Eriobotrya japonica* Leaves Reduces Glucose Level in Human Hepatocellular Carcinoma Cells, Zebrafish and Rats," *Scientific Reports* 9 (2019): 1–13.
5. P. B. Kasangana, P. S. Haddad, H. M. Eid, A. Nachar, and T. Stevanovic, "Bioactive Pentacyclic Triterpenes From the Root Bark Extract of *Myrianthus arboreus*, a Species Used Traditionally to Treat Type-2 Diabetes," *Journal of Natural Products* 81 (2018): 2169–2176, <https://doi.org/10.1021/acs.jnatprod.8b00079>.
6. H. Sharma, P. Kumar, R. R. Deshmukh, A. Bishayee, and S. Kumar, "Pentacyclic Triterpenes: New Tools to Fight Metabolic Syndrome," *Phytomedicine* 50 (2018): 166–177.
7. R. de la Torre, M. Carbó, M. Pujadas, et al., "Pharmacokinetics of Maslinic and Oleanolic Acids From Olive Oil—Effects on Endothelial Function in Healthy Adults. A Randomized, Controlled, Dose-Response Study," *Food Chemistry* 322 (2020): 126676.
8. A. Khan, A. H. Shah, and N. Ali, "In-Vitro Propagation and Phytochemical Profiling of a Highly Medicinal and Endemic Plant Species of the Himalayan Region (*Saussurea costus*)," *Scientific Reports* 11 (2021): 23575.
9. H. N. Murthy, E. J. Lee, and K. Y. Paek, "Production of Secondary Metabolites From Cell and Organ Cultures: Strategies and Approaches for Biomass Improvement and Metabolite Accumulation," *Plant Cell, Tissue and Organ Culture* 118 (2014): 1–16.
10. D. Cochran and R. Powers, "Fourier Transform Ion Cyclotron Resonance Mass Spectrometry Applications for Metabolomics," *Biomedicine* 12, no. 8 (2024): 1786.
11. M. Maia, A. Figueiredo, C. Cordeiro, and M. Sousa Silva, "FT-ICR-MS-Based Metabolomics: A Deep Dive Into Plant Metabolism," *Mass Spectrometry Reviews* 42 (2023): 1535–1556, <https://doi.org/10.1002/mas.21731>.
12. P. H. Canter, H. Thomas, and E. Ernst, "Bringing Medicinal Plants Into Cultivation: Opportunities and Challenges for Biotechnology," *Trends in Biotechnology* 23 (2005): 180–185.
13. G. L. Montoya Peláez, J. A. Sierra, F. Alzate, U. Holzgrabe, and J. R. Ramirez-Pineda, "Pentacyclic Triterpenes From *Cecropia telenitida* With Immunomodulatory Activity on Dendritic Cells," *Revista Brasileira de Farmacognosia* 23 (2013): 754–761.
14. N. A. Hazzi, J. S. Moreno, C. Ortiz-Movliav, and R. D. Palacio, "Biogeographic Regions and Events of Isolation and Diversification of the Endemic Biota of the Tropical Andes," *Proceedings of the National Academy of Sciences of the United States of America* 115 (2018): 7985–7990.
15. G. Gutiérrez, L. M. Valencia, D. Giraldo-Dávila, et al., "Pentacyclic Triterpene Profile and Its Biosynthetic Pathway in *Cecropia telenitida* as a Prospective Dietary Supplement," *Molecules* 26 (2021): 1–14.
16. C. Mosquera, A. Panay, and G. Montoya, "Pentacyclic Triterpenes From *Cecropia telenitida* Can Function as Inhibitors of 11 β -Hydroxysteroid Dehydrogenase Type 1," *Molecules* 23 (2018): 1444.
17. D. F. Smith, D. C. Podgorski, R. P. Rodgers, G. T. Blakney, and C. L. Hendrickson, "21 Tesla FT-ICR Mass Spectrometer for Ultrahigh-Resolution Analysis of Complex Organic Mixtures," *Analytical Chemistry* 90 (2018): 2041–2047.
18. M. L. Chacón-Patiño, R. Moulian, C. Barrère-Mangote, et al., "Compositional Trends for Total Vanadium Content and Vanadyl Porphyrins in Gel Permeation Chromatography Fractions Reveal Correlations Between Asphaltene Aggregation and Ion Production Efficiency in Atmospheric Pressure Photoionization," *Energy and Fuels* 34 (2020): 16158–16172.
19. K. Miettinen, S. Iñigo, L. Kreft, et al., "The TriForC Database: A Comprehensive Up-to-Date Resource of Plant Triterpene Biosynthesis," *Nucleic Acids Research* 46 (2018): D586–D594.
20. E. Bae, I. J. Yeo, B. Jeong, Y. Shin, K. H. Shin, and S. Kim, "Study of Double Bond Equivalents and the Numbers of Carbon and Oxygen Atom Distribution of Dissolved Organic Matter With Negative-Mode FT-ICR MS," *Analytical Chemistry* 83 (2011): 4193–4199.
21. B. Rhourri-Frih, P. Chaimbault, B. Claude, C. Lamy, P. André, and M. Lafosse, "Analysis of Pentacyclic Triterpenes by LC-MS. A Comparative Study Between APCI and APPI," *Journal of Mass Spectrometry* 44 (2009): 71–80.
22. S. Ghosh, "Triterpene Structural Diversification by Plant Cytochrome P450 Enzymes," *Frontiers in Plant Science* 8 (2017): 1886.
23. Y. Li, J. Wang, L. Li, et al., "Natural Products of Pentacyclic Triterpenoids: From Discovery to Heterologous Biosynthesis," *Natural Product Reports* 40 (2023): 1303–1353, <https://doi.org/10.1039/d2np00063f>.
24. M. Z. Fanani, E. O. Fukushima, S. Sawai, et al., "Molecular Basis of C-30 Product Regioselectivity of Legume Oxidases Involved in High-Value Triterpenoid Biosynthesis," *Frontiers in Plant Science* 10 (2019): 1520.

25. T. Hoshino, T. Abe, and M. Kouda, "Unnatural Natural Triterpenes Produced by Altering Isoleucine Into Alanine at Position 261 in Hopene Synthase and the Importance of Having the Appropriate Bulk Size at This Position for Directing the Stereochemical Destiny During the Polycyclization Cascade," *Chemical Communications* 6 (2000): 441–442, <https://doi.org/10.1039/b000711k>.
26. F. Hernández-Epigmenio, M. D. García-Mateos, E. Sosa-Montes, et al., "Phenolic Profile and Nutritional Value of *Dahlia xhortorum* Flowers," *Revista Chapingo. Serie Horticultura* 28 (2022): 161–174.
27. M. Behr, G. Neutelings, M. El Jaziri, and M. Baucher, "You Want it Sweeter: How Glycosylation Affects Plant Response to Oxidative Stress," *Frontiers in Plant Science* 11 (2020): 571399.

Supporting Information

Additional supporting information can be found online in the Supporting Information section.